

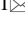
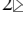



# Wedge stability analysis in fractured soft rock slopes for different orientations of seismic components

Rhita Bennouna<sup>1\*</sup> , Latifa Ouadif<sup>1</sup> , Ahmed Akhssas<sup>1</sup> ,  
Ahmed Skali Senhaji<sup>2</sup> , Ghizlane Boulaid<sup>1</sup> 

<sup>1</sup> Mohammadia School of Engineers, Mohammed V University in Rabat, Rabat, Morocco

<sup>2</sup> Setec Maroc, Rabat, Morocco

\*Corresponding author: e-mail [bennounarhita@gmail.com](mailto:bennounarhita@gmail.com)

## Abstract

**Purpose.** This paper focuses on the case of a rock slope in the Ouarzazate region in order to conduct a sensitive analysis to study the influence of seismic action orientations on wedge stability.

**Methods.** To examine the wedge stability, a probabilistic approach related to the Monte Carlo method has been used. Firstly, the characteristics of joint families: orientations and fillings are analysed. Then, the influence of the seismic action on the rock slope stability for the most sensitive plunges is studied using the equations developed by J. Bray (1981). These equations make it possible to ultimately determine the safety factor for predicting the stability of the wedge.

**Findings.** In this study, the ranges of values of the seismic action orientations leading to the rock wedge failure have been identified. Especially around the 284° trend, the minimum of the safety factor values have been obtained for different analyzed plunges. This means that the occurrence of an earthquake oriented at 284° and lateral to the slope disposition, oriented at 260°, gives rise to a risk of a slope failure.

**Originality.** This study of rock slope stability made it possible to find the minimum safety factor values depending on the orientation of the seismic action by examining its sensitivity to all possible orientations: combinations of plunges and trends.

**Practical implications.** This analysis makes it possible to find, whatever the orientation of the seismic action, the safety factor corresponding to the stability of the rock slope. Thus, a decision can be made on the appropriate reinforcement to ensure the rock slope stability, taking into account the case of the most unfavourable seismic action orientation found in this analysis.

**Keywords:** stability, seismicity, joints, plunge, trend, safety factor, fracturing

## 1. Introduction

For a long time, numerous researches have been carried out on the rock mass stabilization based on the various developed methods. The characteristics of rock slopes, the presence of sensitive adjoining structures make the stabilization of the rock slope a priority task. This is especially true, since the damages caused by a slope failure are numerous and economically heavy, which fully justifies the need to identify and strengthen unstable rock slopes. The presence of groundwater leads to pore pressure. The seismicity of the study area, climatic conditions, overloads and any external stress, combined with the presence of families of joints, are factors that significantly influence the slope stability. In order to ensure *optimal safety against landslides* and large rock falls, it is necessary to carry out *risk mapping* and identify unstable areas [1], and then proceed to treatment by zones; each zone represents a specific case that needs to be reinforced (nailing, shotcrete, dynamic barrier, rockfall netting hanging, tie rods, ...). A meticulous *analysis of the rock mass characteristics* helps to better understand the rock behaviour [2].

The first step that needs to be taken to do this is *the rock mass characterization*. The intensity of rock fracturing strongly influences its overall resistance, and, therefore, the rock mass behaviour [3]. This parameter correlates with the intact rock compressive strength, whether the *point load strength index* or the *uniaxial compressive strength* is known. It also correlates with the drill core quality rating (RQD), with the discontinuity spacing, the discontinuity conditions and the groundwater influence in the rock to characterize the studied rock formation. Many researchers around the world have directed their researches in this way in order to find an ideal correlation for characterizing rock masses and assessing the underground stability, in particular the RMR: Rock Mass Rating [4] and the Q-system [5]. Furthermore, correlations between these parameters have been made [6] and some adjustments have been developed to allow the classification to be applied to rock slopes. Of these, in particular, the Slope Masse Rating (SMR) [7], the Chinese slope mass rating (CSMR) based on SMR [8], SMR continuous slope mass rating [9], representing continuous functions of the factors included in the constitution. As the basic equation for SMR, the graphical SMR [10], which includes the stereo plot repre-

Received: 29 November 2022. Accepted: 28 May 2023. Available online: 30 March 2024

© 2024. R. Bennouna, L. Ouadif, A. Akhssas, A.S. Senhaji, G. Boulaid  
Mining of Mineral Deposits. ISSN 2415-3443 (Online) | ISSN 2415-3435 (Print)

This is an Open Access article distributed under the terms of the Creative Commons Attribution License (<http://creativecommons.org/licenses/by/4.0/>), which permits unrestricted reuse, distribution, and reproduction in any medium, provided the original work is properly cited.

sentation, and the Hazard index (HI), which takes into account the rock normal conditions, as well as the instability of trigger mechanisms [11] can be mentioned. In different rock formation analysis methods mentioned above, it can be observed that they mainly consider the state of joint families present in the rock taking into account their dips and dip directions, as well as by analysing the intersection line of joints and rock slope dip.

This paper is focused on slope rock masses. It is obvious that the failure mechanisms of slopes occur either by circular slip, by plane sliding, by wedge sliding or by toppling. They usually occur quite quickly and the analysis of these types of landslides requires a rock fracture characterization. As for wedge slip failures, they can occur over a wide spectrum of geological and geometric conditions and have been widely discussed in the geotechnical literature by [12]-[16] and many other researchers. Three-dimensional analyses were carried out in order to delineate the unstable wedge for each study case depending on the rock fracturing, as well as the cohesion and friction angle of the discontinuity planes, which significantly influence the slope stability. This analysis will be applied to an area located in the Moroccan Central High Atlas which is characterized by a Paleozoic basement and a Triassic-Zurassic cover, and more specifically in the Tichka area.

This study will assess the wedge stability under seismic action impact. A sensitivity study is conducted to measure the importance of the seismic action impact on the block stability, highlighting the influence of cohesion and friction angle along all the joint fractures.

## 2. Methods

### 2.1. Location of the study area

The road embankment that we have chosen to study is located at the edge of a road built in High Atlas mountainous area, forming small very sharp bends. These mountain slopes have very steep dips. The construction of this road was very important in creating a link between the south-eastern part and the other parts of Morocco.

This is the Tizi n'Tichka Pass section, which culminates in the highest mountain peaks both on the scale of this road and on a national scale. The Tizi n'Tichka Pass is located 100 km from the city of Marrakech and 5 km south-east of the village of Tadarte (Fig. 1a, b).

This pass, built at an altitude of 2300 m, is the highest section of the national road RN09. It connects Marrakech with Ouarzazate at a distance of 200 km. The route of this pass contains very sharp bends, crossing fractured schist formations, the hardness of which increases with depth.

### 2.2. Methods for assessing the rock slope stability

To assess the degree of the entire section instability, several field missions were carried out to locate the studied route in a regional and local geological context, describe the lithological column of each zone and conduct a structural survey of the study area. A probabilistic approach using the Monte Carlo method allows examining the variability effect of each parameter on slope stability. Compared to the deterministic approach, which presents one and only one safety factor that can be stable or not, related to fixed and determined input parameters, this approach offers a probability distribution of the safety factor, thus presenting an interval of the safety factor values and allowing to identify the probability of slope failure.

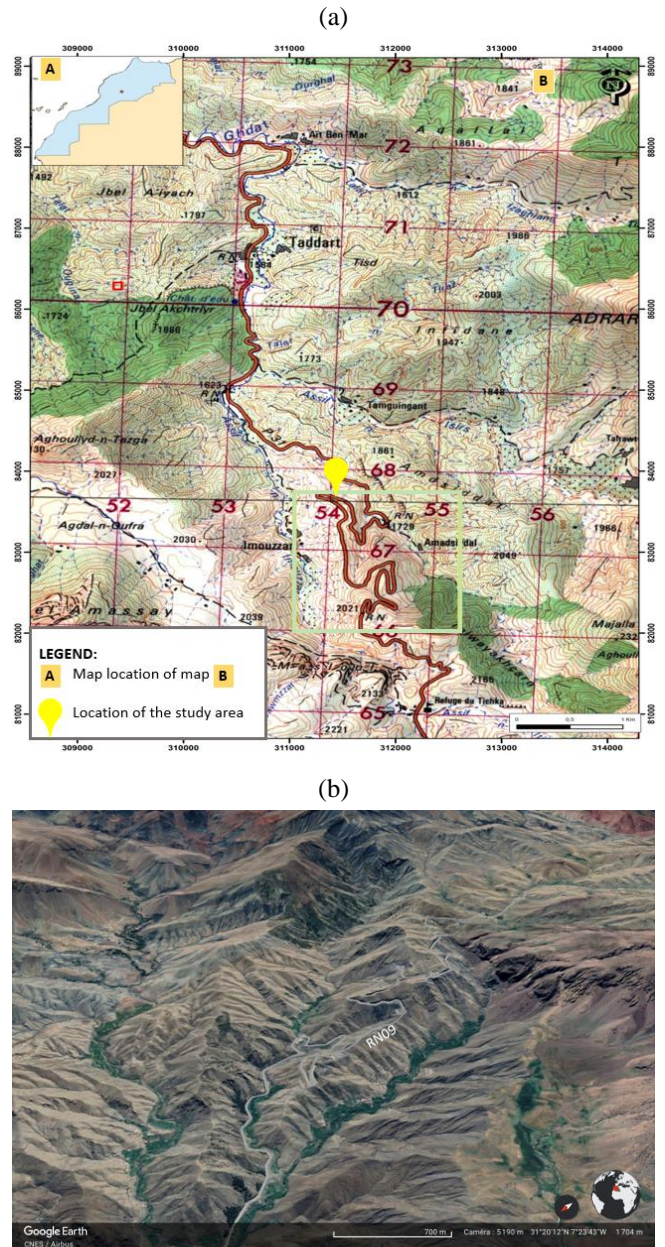


Figure 1. Tizi n'Tichka pass: (a) location on the Had Zraqtane 1/50000 topographic map; (b) three-dimensional google earth satellite image

It is clear that the probability of failure will be calculated in the same way as that of the safety factor, taking into account the resisting and driving forces.

It is a realistic method, widely used in rock mechanics and engineering, providing access to the management of uncertainties due to heterogeneities associated with rock composition, porosities and cracks, as well as any other parameters representing a spectrum of values [17]-[19]. It is necessary, when examining the risk of rock mass instability, to take into account the variability of parameters, which makes the analysis more logical and realistic [20]. However, in order to get as close as possible to reality, the approach proposes to model the parameters as probability density functions. We can distinguish different types: normal, uniform, triangular, beta, exponential, lognormal distributions (Example in engineering) [21]. The normal distribution, which is also the most frequently used, presents the mean value as the most frequent value of the studied parameter [19]. In terms of this approach, two



methods are proposed for calculating the reliability coefficient, namely, the margin safety and the Monte Carlo methods. The second method offers versatility and good analysis accuracy. Whatever the combinations of functions adopted for the parameters and the interdependence or lack of interdependence of these parameters, this method resolves different operations. It is also the most frequently used method in probabilistic approach researches [22]-[24].

### 2.3. Stereographic representation of structural geology data

Stereographic data representation is a crucial step in understanding the structural geology of a rock mass. Having identified the different families of existing joints, it is important to determine whether their collective presence could pose a potential risk to slope stability (risk of circular, plane, wedge or overturning slips). It is for this reason that this graphic representation offers the possibility of locating the poles representing dip and dip direction of each set of discontinuities, forming a cloud of points that can be interpreted on the graph and identify the nature of the instability and sliding direction [25]. In addition, the dip and the dip direction of the joint intersection lines can be identified on the stereonet. It is also possible to determine on the stereonet the joint orientation compared to the face slope, and the upper face, if it exists, which can also be represented on the stereonet. The steps for constructing dips and dip direction, reading and interpretation of stereonets are described in detail in the 4th edition of *Rock Slope Engineering: Civil and Mining* [26], based on the 3rd edition by E. Hoek and J. Bray.

In order to carry out a rock slope stability study, it is important to carry out a stereographic representation [27], since it constitutes the basis of the analysis making it possible to assimilate the phenomenon of fracturing in the slope before starting the actual study.

### 2.4. Rock slope stability analysis

Reading the plots on the stereonets makes it possible to identify the instability nature that may occur in the case of an embankment. In order to confirm this graphical reading and quantify this instability, comparison of joint dips and dip directions, as well as the various resistance and driving factors related to the slope, allow us to identify the degree of slope stabilization. It is important to note that the rock slope dip and the joint filling have a major impact on the stability.

In the case of wedge failure, when the planes of discontinuities intercept the slope face obliquely, the wedge shape is delimited by five faces distributed as follows (Fig. 2):

- two sliding surfaces 1 and 2, including their intersection line;
- the slope upper face 3;
- the slope main face 4;
- the extension surface of tension crack (if it exists) 5.

In addition to the discontinuity orientations noted on the slope, other destabilizing factors may arise (presence of water, seismic stresses, external stresses, presence of a tension crack), which can significantly reduce the safety factor. However, it is important to note that solving the equations to find the safety factor becomes more tedious when adding any factor having an influence on stability. These equations were developed by [28] taking into account the input parameters: joint orientations; wedge shape; wedge weight; water pressure; seismicity effect; shear strength at the surface planes; any external solicitation; the impact of any stabilizing treatment (active or passive anchoring, for example).

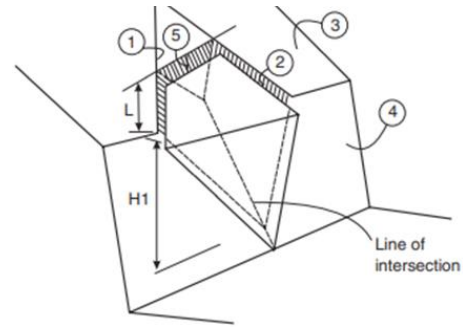


Figure 2. Surfaces defining the wedge shape [26]:  $H_1$  – the vertical height between the point where the intersection line daylight on the face and the intersection of plane 1 with the slope crest;  $L$  – the distance measured along plane 1 between the crest of the slope face 4 and the tension crack 5

The equations developed below take into account all the stresses and conditions mentioned above, given that this is indeed the case of a tetrahedral wedge bounded by five surfaces listed above.

The safety factor is calculated as follows:

$$FS = \frac{Q}{S}, \quad (1)$$

where:

$FS$  – factor of safety;

$Q$  – total shear resistance on planes 1 and 2;

$S$  – total shear force on planes 1 and 2.

Two notions are introduced:  $N_1$  and  $N_2$ , representing effective normal reactions on planes 1 and 2, the calculation of which is based on a series of developed equations, based on dips and dip direction data of the joint surface, the upper slope, the face slope, wedge weight and shape, as well as various stresses. Any parameter change will influence the values of these effective normal reactions:

$$N_1 = \rho(Wk_z + T(rv - s) + E(rv_e - s_e) + V(rv_5 - s_5)) - u_1 A_1; \quad (2)$$

$$N_2 = \mu(Wl_z + T(rs - v) + E(rs_e - v_e) + V(rs_5 - v_5)) - u_2 A_2. \quad (3)$$

Moreover, by identifying the sign of the numerical values  $N_1$  and  $N_2$  (higher or lower than 0), it is possible to determine whether contact is maintained on a single sliding surface, on two surfaces, or contact is lost on both planes.

For each case of contact, particular expressions  $Q$  and  $S$  are clarified in order to find the safety factor characteristic of this case.

In the case when  $N_1 > 0$  and  $N_2 > 0$ , we obtain the following:

$$Q = N_1 \tan \phi_1 + N_2 \tan \phi_2 + c_1 A_1 + c_2 A_2; \quad (4)$$

$$S = v(Wi_z + T\omega + E\omega_e - V\omega_5), \quad (5)$$

where:

$c_1 A_1$  and  $c_2 A_2$  – cohesive force of sliding surfaces;

$W$  – wedge weight;

$T$  – anchoring tension;

$E$  – external loading;

$V$  – water pressure at the level of the stress crack.

All other terms of the equations below are equations based on calculations derived from data relating to the dips and dip directions of the slide surfaces, upper face and the slope face.

It is not systematic to have all of the above elements grouped together in one study case. However, the equations

are adaptable to each studied wedge. The calculations of the safety factor are detailed in Appendix III of the 4th edition of Rock Slope Engineering Civil and Mining.

### 2.5. Seismicity effect on the slope stability

Most of instabilities are triggered by moderate to high magnitude earthquakes. The state of slope stability before any earthquake should also be taken into account. At the limit of slope equilibrium, even a moderate earthquake magnitude can be enough to trigger instability. In order to understand the relationship between the earthquake magnitude, the location of the source and the risk of instabilities, it is important to analyse a lot of land movements triggered by earthquakes. Keefer has made a correlation between these parameters according to land movements that occurred between 1811 and 1980 [29].

Two inertia forces are determined by usual static methods for determining seismic force:

$$F_H = \alpha_H \cdot Q ; \tag{6}$$

$$F_V = \pm \alpha_V \cdot Q , \tag{7}$$

where:

$F_H, F_V$  – in the horizontal and vertical directions, respectively;  
 $Q$  – soil element weight increased by the load applied to it;  
 $\alpha_H, \alpha_V$  – seismic coefficients;  $\alpha_H$  – is expressed as a function of the nominal acceleration  $a_n$  and the acceleration  $g$ .

To measure the influence of the formation geological nature on the amplification of maximum horizontal acceleration, a correlation obtained with different values is plotted in the graph below (Fig. 3) [30].

In our study we are interested in the case of rock layers. The graph shows that when an earthquake occurs, wave propagation depends on the nature of geological formations being crossed; its impact is relatively weakened within hard formations compared to soft formations. Fortunately, geological rock formation has lower amplification factor than soil with low or no cohesion.

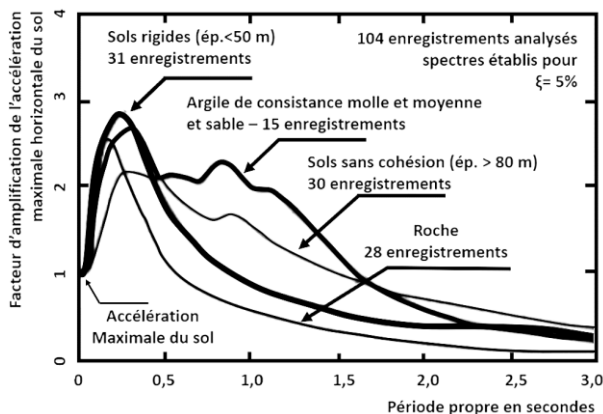


Figure 3. Influence of soil nature on the amplification factor [30]

In addition, the value of the inertial forces should be taken into account due to its sensitive influence on the local rock mass stability. A study conducted in [31] shows that since the horizontal coefficient  $\alpha_H$  is the most important component of seismic action, an increase in coefficient  $\alpha_H$  with an increment in 0.1 for different rock slope angles significantly decreases the safety factor value of the slope and increases the risk of failure.

## 3. Results and discussion

### 3.1. Characteristics of the joint families

Concerning fracturing planes, this structure is affected by three main fracture families summarized in Table 1.

Table 1. Dip and dip direction of joint families

Joint families	Dip	Dip direction	Joint spacing, m
S1	N15 to N25	60 to 85° W	2 to 3
S2	N85	90° S	2
S3	N135 to N140	60° SW	0.50

Slope failure occurs if the geometric configurations of the slope and discontinuities allow it. A risk of failure exists if these configurations lead to a kinematically possible rupture.

### 3.2. Stereographical representation

Identification of the risk of failure of an elementary rupture mechanism is based on comparing the angles of different discontinuities and the slope angles. The use of stereographic projection diagrams makes it possible to highlight geometric configurations leading to rupture [28].

The cross of large circles shows that there are intersection lines between the joint families. Each intersection line is characterized by two parameters: plunge and trend. In this case, we notice that there are three intersection lines that are combinations of couples of every joint family (Fig. 4). Generally, the orientation of the intersection lines shows the direction of sliding, and the angles formed between the planes indicate the wedging action where the planes intersect. The presence of this intersections of lines with a slope, when the dip and dip direction are equal to (N180; 72° W), respectively, can form a wedge for which stability should be analysed.

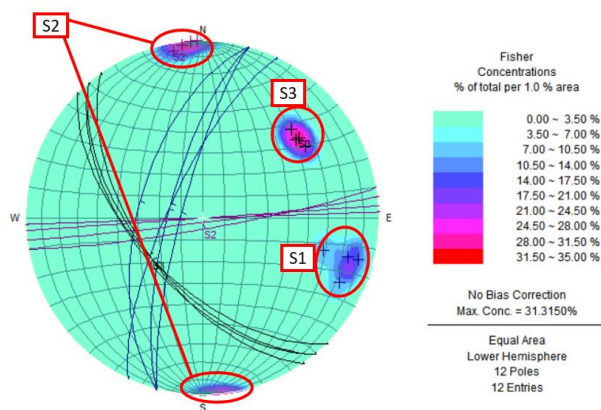


Figure 4. Spatial distribution of discontinuities

It is important to take into account the filling materials of the joint planes. Joint opening, cohesive and frictional properties of rock discontinuities have a direct effect on the rock mass shear strength, especially when detrital material is the filler. Table 2 summarizes the nature of filling materials and the joint opening size for each discontinuity surface.

Table 2. Joint filling nature and joint opening size

Joint families	Joint filling	Joint opening size, cm
S1	Shale	2 to 3
S2	Sliced shale	1.5
S3	Shale	1.5 to 2

In rock masses, failure can develop especially on discontinuity planes that have weaker mechanical characteristics than those of the rock matrix, causing the rock mass sliding along one or more fracture planes. In this case, the cohesion of materials on discontinuity planes is estimated at 1.5 t/m<sup>2</sup> and the friction angles at 20°. These values are significantly lower than rock mass properties, which jeopardizes the block stability.

Assuming that failure can only occur along fractures, the failure surfaces will depend only on the network of rock mass fracturing. Depending on this network, one or more kinematically possible failure mechanisms are determined. Force or moment balance leads to a safety factor calculation.

### 3.3. Stability analysis

This study is focused particularly on the impact of seismic component action on the slope stability. This component is represented by horizontal and vertical acceleration coefficients.

According to site study, the maximal acceleration is 0.1 g with:

$$\alpha_H = 0.5 \cdot \alpha \cdot S = 0.05 ; \tag{8}$$

$$\alpha_V = \pm \frac{1}{3} \cdot \sigma h = 0.017 . \tag{9}$$

When  $\alpha = ag / g = 0.1$ ,  $S$  is soil parameter that is equal to 1 (for rock formation with a less resistant superior layer).

#### 3.4.1. Impact of joint plane parameters on the slope safety factor for various coefficients of seismic forces

Under the action of seismic waves of different intensity, the earthquake can cause potential rock slope disasters. Many studies have been developed in this way [32]-[34], and some experimental laboratory tests have been conducted for earthquake simulation to analyse the impact on rock bedding slope [35].

The seismic action has an impact on the rock mass stability, and its action depends closely on the rock mass parameters. A rock mass with low cohesion associated with seismic action will lead to a very low safety factor for different friction angle values (even if there is a sensitive fluctuation of the  $FS$  according to its values). The graphs below are plotted considering a seismic action plunge of 0°, which results in a minimal safety factor value (compared to the plunges towards the intersection of joint families), and which will be shown later, as well as 285° trend. These graphs show that the safety factor values will be lower with an increase in the seismic action component even for a cohesive rock formation. It is true that stability is ensured for good cohesive slopes with different values of friction angles and seismic action less or equal to 0.2 (Fig. 5a, b, c). Nevertheless, an important seismic action can lead to a decrease in  $FS$  and slope instability.

The safety factor varies depending on the importance of the seismicity action in the study area. It should be noted that a low seismicity coefficient value can clearly provide better stability of the slope under study. Based on this analysis and passing from one seismic coefficient to another with an increment in 0.1, we notice the difference between their respective safety factors, where, of course, an inverse proportionality can be found. In addition, when the friction angle is important, relatively high safety factor values are achieved (the values obtained obviously depend on each case study).

The following graph (Fig. 6) shows that the influence of the friction angle on the safety factor gradually decreases at high seismicity coefficient values.

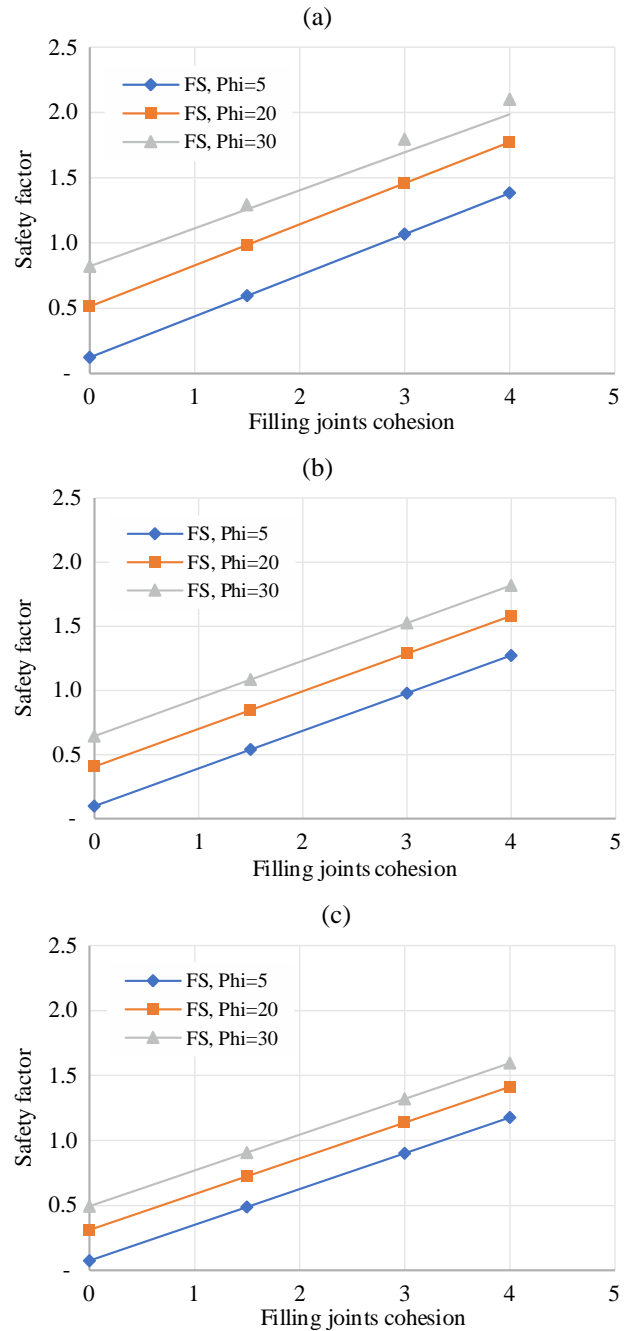


Figure 5. Safety factor variation for different values of cohesion with sensitive values of the seismic component action: (a) without seismic component; (b) with seismic component equal to 0.1; (c) with seismic component equal to 0.2

In this analysis, the cohesion value is 1.5 t/m<sup>2</sup>, which is similar to the joint filling cohesion of the study project and underlines the presence of rock slope instability regardless of the seismic coefficient value.

In this study case, the cohesion  $C$  is equal to 1.5 t/m<sup>2</sup>, the friction angle  $\phi$  is 20° and seismic coefficient is 0.1.

Considering the zero plunge and 284° trend, which represent the most unfavourable case for stability, and knowing the values of cohesion and friction angle, as well from an interval of values for the dip/dip direction of the different joint families (Table 1), we obtain the graph Figure 7, representing the frequency of distribution of the safety factors found using the adopted probabilistic approach.



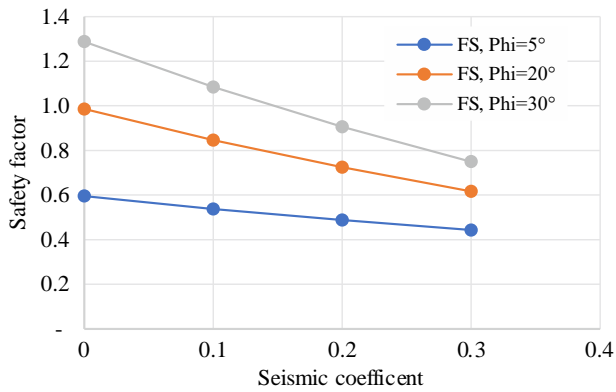


Figure 6. Variation of the safety factor for seismic coefficient increment for different friction angle values and a fixed cohesion value of 1.5 t/m<sup>2</sup>

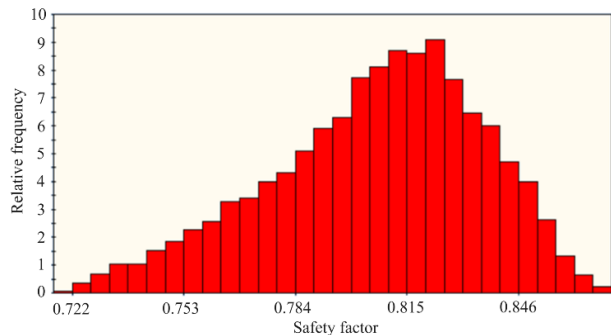


Figure 7. Histogram of the safety factor occurrence frequency

### 3.4.2. Influence of the seismic action plunge and trend on the rock slope stability

It is known that the seismic action is decomposed into two actions (horizontal and vertical components). The orientation of these actions can be in any plunge. Given that the horizontal component is the most important, we obtain relatively reduced plunge values.

Since the wedge formation at the rock slope level, defined as following a fracturing system, is exposed to a risk of instability for various reasons (water pressure, seismicity, etc.), it is important to assess the degree of its instability. Using the equations developed by Hoek and Bray, presented previously, we can find the safety factor, which depends on many parameters. We will focus in this part on the impact of the seismic action orientation on the block stability.

The analysis consists in studying the application of a seismic acceleration of 0.1 in horizontal orientation for different trends and then varying the plunge to determine where seismicity has a considerable impact on the safety factor.

The most sensitive plunges that will be analysed are: horizontal action only (0° plunge) and plunges at the intersection of two by two joint families. The analysis of different fracturing families has revealed the following data related to the intersection of discontinuity planes (Table 3).

Table 3. Plunge and trend values for the intersection lines of different joint families

Joint families	S1 & S2	S2 & S3	S1 & S3
Line of intersection plunge	79.37°	53.00°	59.38°
Line of intersection trend	265°	265°	212.34°

Calculation of safety factors for all possible orientations in different case studies provides a graph in Figure 8.

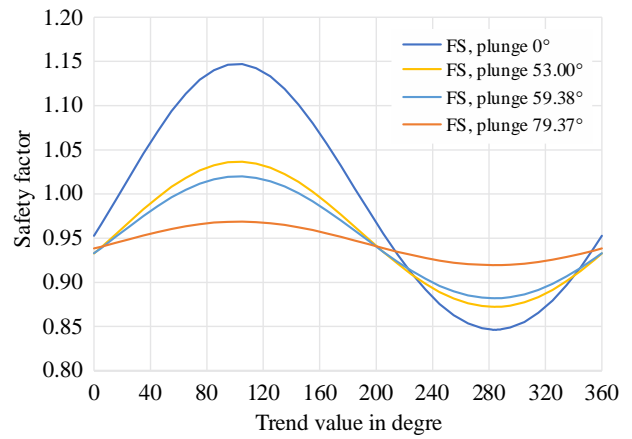


Figure 8. Evolution of the safety factor for different plunge and trend values

From the graph we can observe that by varying the trend over 360°, possible for any plunge, the FS values oscillate in a sinusoidal way following two distinct functions specific to each plunge value. We focused on this analysis as the pessimistic case for a plunge of 0° and obtained the following function:

$$f(x) = 0.19416 \cdot \sin\left(0.8726x \cdot \frac{\pi}{180}\right) + 0.9528; \quad (10)$$

$$0^\circ < x < 206.28^\circ;$$

$$f(x) = 0.10644 \cdot \sin\left(1.17096\left(x \cdot \frac{\pi}{180} - 2\pi\right)\right) + 0.9528; \quad (11)$$

$$206.28^\circ < x < 360^\circ.$$

In addition, the analysis shows that the greater the plunge of the seismic action, the more the risk and/or the importance of the rock slope instability is reduced. For all analysed critical orientations, there is always a risk of instability, especially in the trend interval, which widens with increasing seismic action inclination angle (Table 4). However, from a plunge of 68°, we no longer obtain the stability of this rock slope, no matter where the trend of the seismic action is applied. The plunge relative to the intersection line of joint families 2 and 3 is a part of this plunge range, giving rise to an insured instability.

Table 4. Trend interval of rock slope instability for different plunges

Plunge, °	Interval of trends leading to instability
0	[0°, 18°] & [188°, 360°]
53.00	[0°, 48°] & [158°, 360°]
59.38	[0°, 59°] & [146°, 360°]
79.37	[0°, 360°]

This analysis made it possible to highlight critical trend values that lead to a drop in the safety factor value (Table 4). In the area of 284° trend, we obtain the minimum of FS values for the plunges 0, 53.00, 59.38, 79.37°, which are equal to: 0.846, 0.872, 0.882, and 0.919, respectively.

This shows that the occurrence of a 284° earthquake, located laterally to the slope disposition, which is oriented at 260°, gives rise to an insured instability and a risk of a slope failure.

The analysis also shows that by varying the FS with different trends, it is possible to obtain the most optimal case of security, which is nothing more than the trend opposite to that where the FS is minimal: trend 105°. We can then notice

that the *FS* values are complementary to the opposite trend values. This observation is evident from the fact that during an earthquake, seismic waves propagate and orient in the direction of the trend and in the opposite direction, in the same plunge. For waves in the trend direction, the *FS* value reduces and instability is likely to occur, while for waves in the opposite trend, they lead to improved wedge stability.

Knowing the *FS* average sum and the *FS* of a trend allows determining the *FS* at the opposite trend. The trend curve plotted on the graph (Fig. 9) gives the equation below:

$$Y = -0.0013x + 1.9787. \tag{12}$$

This curve shows that the greater the plunge, the more we obtain an average value of the sum of safety factor for two opposite trends that become increasingly weak, in addition to a gradual decrease in the maximum amplitude of the curve representing the plunge oscillations for different trends (Fig. 9).

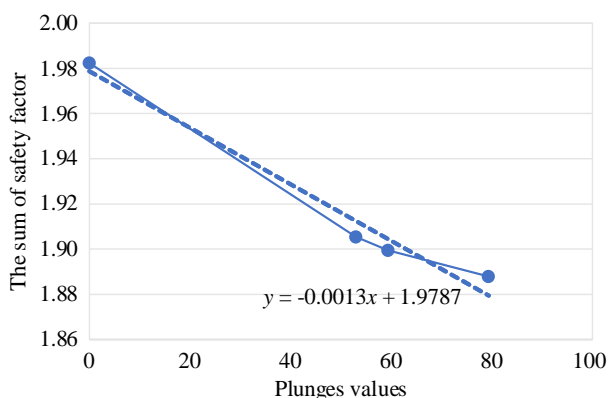


Figure 9. Arithmetic mean of the sum of safety factors of opposite trends for different plunge values

As the previously obtained function is not unique, the average value around which the safety factors oscillate for different trends is not equal to the average value of any of the two oscillation functions (Table 5). But rather, the average *FS* oscillation can be obtained by subdividing the arithmetic mean of the sum of *FS* by 2, with an approximate error up to 2%.

Table 5. Specific values for arithmetic mean of the sum of opposite trend safety factors for horizontal plunge, seismic action plunge, and different lines of joint intersection plunges

Plunge	0°	53°	59.38°	79.37°
Arithmetic mean of the sum of opposite trend safety factors	1.9823	1.9054	1.8995	1.8879

This drop in the arithmetic mean of the *FS* sum with changing plunges, observed in the curve above, and in addition to decreasing continually amplitude maximum oscillations, shows that from a certain plunge value the mean oscillation value will be reduced so much that it will give rise to the rock block instability regardless of the seismic action direction. This aligns with the results of the analysis, developed previously, which showed that the critical plunge is 68°.

#### 4. Conclusions

One of the major factors that should be taken into account when studying the rock slope stability is the site seismicity. We sometimes find a weak seismicity in a zone without taking into account the impact, even weak, on the stability of

the rock blocks. It is observed that throughout this study, the seismic coefficient value has different oscillations depending on its orientation: its plunge and its trend, the value of the plunge is known in advance. Each zone is a particular case study, so the focus on our case study has highlighted the values of critical trends in seismic action giving rise to certain instabilities, regardless of the plunge value along which this action is applied.

The presence of joint families with different plunges and trends that could fall within the range of critical values would give rise to wedge instability formed by these joints. A stringent analysis of joint orientation has revealed that if seismic action is applied at one of the intersections of already known joint families, then we would have insured instability. But since the seismic action is applied towards a plunge, and the trend is not known, there is then a risk of instability which strongly depends on the trend value with an instability interval.

By following the method of probabilistic analysis, we will find an interval of safety factor values for the wedge stability. Therefore, the frequency of the seismic action will not be a fixed value, but rather specific to each combination of joint family orientations that allow to obtain a matrix of values containing the safety factor distribution, which can be analysed according to the predominance of the joint orientations.

#### Author contributions

Conceptualization: RB, LO, AA; Data curation: RB; Formal analysis: RB; Investigation: RB, ASS, GB; Methodology: RB, LO, AA, ASS, GB; Project administration: RB, ASS; Resources: RB; Software: RB; Supervision: LO, AA; Validation: LO, AA; Visualization: LO, AA; Writing – original draft: RB; Writing – review & editing: RB. All authors have read and agreed to the published version of the manuscript.

#### Funding

This research received no external funding

#### Conflicts of interests

The authors declare no conflict of interest.

#### Data availability statement

The original contributions presented in the study are included in the article, further inquiries can be directed to the corresponding author.

#### References

- [1] Meziane, S., Bahi, L., & Ouadif, L. (2019). Automatic recognition of land instability. *International Journal of Recent Technology and Engineering*, 8(2), 1972-1977. <https://doi.org/10.35940/ijrte.B1967.078219>
- [2] Driouch, A., Ouadif, L., Lahmili, A., & Belmi, M.A. (2022). Evaluation of the compression potential of serpentine rock masses of the Bou Azzer Mining District in the Central Anti-Atlas of Morocco. *Mining, Metallurgy & Exploration*, 39, 189-200. <https://doi.org/10.1007/s42461-021-00517-5>
- [3] Hoek, E. (1983). Strength of jointed rock masses. *Géotechnique*, 23(3), 187-223. <https://doi.org/10.1680/geot.1983.33.3.187>
- [4] Bieniawski, Z.T. (1989). *Engineering rock mass classifications: A complete manual for engineers and geologists in mining, civil, and petroleum engineering*. Pennsylvania, United States: John Wiley & Sons, 250 p.
- [5] Barton, N., Lien, R., & Lunde, J. (1974). Engineering classification of rock masses for the design of tunnel support. *Rock Mechanics and Rock Engineering*, 6(4), 189-236. <https://doi.org/10.1007/BF01239496>
- [6] Driouch, A., Ouadif, L., Lahmili, A., & Belmi, M.A. (2021). Correlation between Q-system and rock mass rating of the serpentine rock mass at the Bou Azzer Mine in the Central Anti-Atlas of Morocco. *Annals of the Romanian Society for Cell Biology*, 25(6), 12726-12733.

- [7] Romana, M. (1985). New adjustment ratings for application of Bieniawski classification to slopes. *Proceedings of the International Symposium on the Role of Rock Mechanics in Excavations for Mining and Civil Works*, 49-53.
- [8] Chen, Z. (1995). Recent developments in slope stability analysis. *Proceedings of the 8<sup>th</sup> ISRM Congress*, 3, 1041-1048.
- [9] Tomás, R., Delgado, J., & Serón, J.B. (2007). Modification of slope mass rating (SMR) by continuous functions. *International Journal of Rock Mechanics and Mining Sciences*, 44, 1062-1069. <https://doi.org/10.1016/j.ijrmms.2007.02.004>
- [10] Tomás, R., Cuenca, A., Cano, A., & Garcia-Barba, J. (2012). A graphical approach for slope mass rating (SMR). *Engineering Geology*, 124, 67-76. <https://doi.org/10.1016/j.enggeo.2011.10.004>
- [11] Pantelidis, L. (2010). An alternative rock mass classification system for rock slopes. *Bulletin of Engineering Geology and the Environment*, 69(1), 29-39. <https://doi.org/10.1007/s10064-009-0241-y>
- [12] Goodman, R.E. (1964) the resolution of stresses in rock using stereographic projection. *International Journal of Rock Mechanics and Mining Science & Geomechanics Abstracts*, 1(1), 93-103. [https://doi.org/10.1016/0148-9062\(64\)90072-5](https://doi.org/10.1016/0148-9062(64)90072-5)
- [13] Wittke, W.W. (1965). *Method to analyse the stability of rock slopes with and without additional loading*. *Rock mechanics and engineering geology*. Vienna, Austria: Springer-Verlag, 52 p.
- [14] Coates, D.F. (1967). *Rock mechanics principles. Energy mines and resources*. Ottawa, Canada: Queen's Printer, 874 p.
- [15] Londe, P., Vigier, G., & Vormeringer, R. (1970). Stability of slopes – graphical methods. *ASCE Soil Mechanics and Foundation Division Journal*, 96(4), 1411-1434. <https://doi.org/10.1061/JSFEAQ.0001446>
- [16] Hudson, J.A., & Harrison, J.P. (1997). *Engineering rock mechanics: An introduction to the principles*. Netherlands: Pergamon Press, 444 p.
- [17] Mollon, G., Dias, D., & Soubra, A.H. (2009). Probabilistic analysis and design of circular tunnels against face stability. *International Journal of Geomechanics*, 9(6), 237-249. [https://doi.org/10.1061/\(ASCE\)1532-3641\(2009\)9:6\(237\)](https://doi.org/10.1061/(ASCE)1532-3641(2009)9:6(237))
- [18] Miro, S., König, M., Hartmann, D., & Schanz, T. (2015). A probabilistic analysis of subsoil parameters uncertainty impacts on tunnel-induced ground movements with a back-analysis study. *Computers and Geotechnics*, 68(4), 38-53. <https://doi.org/10.1016/j.compgeo.2015.03.012>
- [19] Deng, J., Li, S., Jiang, Q., & Chen, B. (2021). Probabilistic analysis of shear strength of intact rock in triaxial compression: A case study of Jinping II project. *Tunnelling and Underground Space Technology*, 111(4), 103833. <https://doi.org/10.1016/j.tust.2021.103833>
- [20] Dohyun, P., Kim, H.M., Ryu, D.W., Choi, B.H., & Han, K.C. (2013). Probability-based structural design of lined rock caverns to resist high internal gas pressure. *Engineering Geology*, 153(GT4), 144-151. <https://doi.org/10.1016/j.enggeo.2012.12.001>
- [21] Oger, J. (2014). *Méthodes probabilistes pour l'évaluation de risques en production industrielle. Modélisation et simulation*. Thèse doctorale. Tours, Français: Université François Rabelais.
- [22] Lu, H., Kim, E., & Gutierrez, M. (2019). Monte Carlo simulation (MCS)-based uncertainty analysis of rock mass quality Q in underground construction. *Tunnelling and Underground Space Technology*, 94, 103089. <https://doi.org/10.1016/j.tust.2019.103089>
- [23] Fattahi, H., Varmazyari, Z., & Babanouri, N. (2019). Feasibility of Monte Carlo simulation for predicting deformation modulus of rock mass. *Tunnelling and Underground Space Technology*, 89, 151-156. <https://doi.org/10.1016/j.tust.2019.03.024>
- [24] Sari, M., Karpuz, C., & Ayday, C. (2010). Estimating rock mass properties using Monte Carlo simulation: Ankara andesites. *Computers & Geosciences*, 36(7), 959-969. <https://doi.org/10.1016/j.cageo.2010.02.001>
- [25] Lahmili, A., Ouadif, L., Akhssas, A., & Bahi, L. (2018). Rock stability analysis – A case study. *MATEC Web of Conferences*, 149, 02072. <https://doi.org/10.1051/mateconf/201814902072>
- [26] Wyllie, D.C., & Mah, C.W. (2004). *Rock slope. Engineering civil and mining*. New York, United States: Spon Press, 431 p. <https://doi.org/10.1201/9781315274980>
- [27] Zerradi, Y., Lahmili, A., & Souissi, M. (2020). Stability of a rock mass using the key block theory: A case study. *E3S Web of Conferences*, 150(2), 03024. <https://doi.org/10.1051/e3sconf/202015003024>
- [28] Hoek, E., & Bray, J. (1981). *Rock slope engineering*. London, United Kingdom: CRC Press, 364 p. <https://doi.org/10.1201/9781482267099>
- [29] Keefer, D.K. (1984). Landslides caused by earthquakes. *Geological Society of America Bulletin*, 95(4), 406-421. [https://doi.org/10.1130/0016-7606\(1984\)95<406:LCBE>2.0.CO;2](https://doi.org/10.1130/0016-7606(1984)95<406:LCBE>2.0.CO;2)
- [30] Seed, H.B., Ugas, C., & Lysmer, J. (1976). Site dependent spectra for earthquake resistant design. *Bulletin of the Seismological Society of America*, (Berkeley), 66(1), 221-243. <https://doi.org/10.1785/BSSA0660010221>
- [31] Karrech, A., Dong, X., Elchalakani, M., Basarir, H., Shahin, M.A., & Regenauer-Lieb, K. (2021). Limit analysis for the seismic stability of three-dimensional rock slopes using the generalized Hoek-Brown criterion. *International Journal of Mining Science and Technology*, 32(2), 237-245. <https://doi.org/10.1016/j.ijmst.2021.10.005>
- [32] Changwei, Y., Jingyu, Z., Jing, L., Wenying, Y., & Jianjing, Z. (2017). *Slope earthquake stability*. Singapore: Springer, 218 p. <https://doi.org/10.1007/978-981-10-2380-4>
- [33] Xu, J., & Yang, X. (2018). Seismic stability analysis and charts of a 3D rock slope in Hoek-Brown media. *International Journal of Rock Mechanics and Mining Sciences*, 112, 64-76. <https://doi.org/10.1016/j.ijrmms.2018.10.005>
- [34] Zhang, W.G., Meng, F.S., Chen, F., & Liu, H.L. (2021). Effects of spatial variability of weak layer and seismic randomness on rock slope stability and reliability analysis. *Soil Dynamics and Earthquake Engineering*, 146, 106735. <https://doi.org/10.1016/j.soildyn.2021.106735>
- [35] Zhang, L., Changwei, Y., Ma, S., Guo, X., Yue, M., & Liu, Y. (2020). Seismic response time frequency analysis of bedding rock slope. *Frontiers in Physics*, 8. <https://doi.org/10.3389/fphy.2020.558547>

## Аналіз стійкості клина в тріщинуватих схилах м'яких гірських порід при різних напрямках сейсмічних компонентів

Р. Беннуна, Л. Уадіф, А. Ахссас, А.С. Сенхаджі, Г. Булайд

**Мета.** Проведення аналізу на чутливість для вивчення впливу напрямків сейсмічної дії на стійкість клина у випадку схилу гірських порід в регіоні Уарзатат.

**Методика.** Для дослідження стійкості клина використовувався імовірнісний підхід, пов'язаний із методом Монте-Карло. По-перше, аналізуються характеристики сімейств стиків, – напрями та наповнення. Потім за допомогою рівнянь, розроблених Дж. Бресем (1981), вивчається вплив сейсмічної дії на стійкість схилу гірських порід для найбільш чутливих занурень. Ці рівняння дозволяють остаточно визначити коефіцієнт запасу міцності для прогнозування стійкості клина.

**Результати.** Виділено діапазони значень напрямків сейсмічної дії, що призводять до руйнування клину гірських порід. Визначені мінімальні значення коефіцієнта запасу міцності в районі тектонічної лінії 284°, що були отримані для різних проаналізованих занурень. Встановлено, що виникнення землетрусу під кутом 284° і латеральніше до розташування схилу, орієнтованого під кутом 260°, створює небезпеку його обвалення.

**Наукова новизна.** Дослідження стійкості схилу гірських порід дозволило вперше знайти мінімальні значення коефіцієнта запасу міцності залежно від спрямованості сейсмічної дії шляхом вивчення його чутливості до всіх можливих напрямків: комбінацій занурень і тектонічних ліній.

**Практична значимість.** Цей аналіз дозволяє визначити, якою б не була спрямованість сейсмічної дії, коефіцієнт запасу міцності, що відповідає стійкості схилу гірських порід. Таким чином, може бути прийнято рішення про відповідне зміцнення для забезпечення стійкості схилу гірських порід, зважаючи на випадок найбільш несприятливої спрямованості сейсмічної дії, що може бути виявлена у цьому аналізі.

**Ключові слова:** стійкість, сейсмічність, з'єднання, занурення, тектонічна лінія, коефіцієнт запасу міцності, тріщинуватість

## Publisher's note

All claims expressed in this manuscript are solely those of the authors and do not necessarily represent those of their affiliated organizations, or those of the publisher, the editors and the reviewers.